1-11-2005

Cutoffs of high-energy plateaux for atomic processes in an intense elliptically polarized laser field

A. V. Flegel
Voronezh State University, Voronezh 394006, Russia

M. V. Frolov
Voronezh State University, Voronezh 394006, Russia

N. L. Manakov
Voronezh State University, manakov@phys.vsu.ru

Anthony F. Starace
University of Nebraska-Lincoln, astarace1@unl.edu

Published in *Journal of Physics B: Atomic, Molecular and Optical Physics*, vol. **38,** no. 1 (14 January 2005), pp. L27–L34. http://www.iop.org/EJ/journal/JPhysB

LETTER TO THE EDITOR

Cutoffs of high-energy plateaux for atomic processes in an intense elliptically polarized laser field

A V Flegel[1], M V Frolov[1,2], N L Manakov[1] and Anthony F Starace[2]

[1] Department of Physics, Voronezh State University, Voronezh 394006, Russia
[2] Department of Physics and Astronomy, The University of Nebraska–Lincoln, Lincoln, NE 68588-0111, USA

Submitted October 2004; published online December 17, 2004

Abstract. We present analytical estimates for high-energy plateau cutoff positions in the spectra of the most common laser-atom processes (above-threshold detachment/ionization, high-harmonic generation and laser-assisted electron-atom scattering) for the case of an elliptically polarized, low-frequency laser field.

Among the most spectacular phenomena in laser-atom physics are the broad, plateau-like structures in the high-energy spectra of strong field processes. These features are well known in multiphoton processes involving bound atomic states (such as high-harmonic generation (HHG) and above-threshold ionization/detachment (ATI/ATD)) [1, 2]; their occurrence has also been predicted recently for laser-assisted electron-atom scattering (LAES) [3]. Plateau effects are most pronounced for linear laser polarization, in which case the extent of the plateau regions (i.e. the plateau cutoffs) for both HHG and ATI have been measured experimentally and agree with results of numerical analyses and classical and quasiclassical (mostly one-dimensional) models [1, 2]; they are given by $(|E_0| + 3.17u_p)$ and $10u_p$ respectively, where $|E_0|$ and u_p are the ionization potential and the ponderomotive shift. For an elliptically polarized field, information on the plateau cutoffs is very sparse [2]: for HHG, an estimate of the cutoff position (see (13) below) was obtained in [4] using an approximate quantum result for the HHG amplitude within a zero-range potential (ZRP) model and in [5] using the semiclassical method for a Gaussian form of the dipole matrix element; general features of plateau effects in ATI/ATD for an elliptically polarized field have been discussed in [6]; plateau structures in LAES for the cases of elliptical and circular polarization have been predicted very recently in [7].

In this letter we present analytical estimates for the extent of high-energy plateaux in ATI/ATD, HHG and LAES for an elliptically polarized field. Our study is based on approximations to exact quantum results for the transition amplitudes within the quasienergy approach [8] for the case of a short-range potential [9, 10]. Detailed analytical study of strong field processes is possible only for short-range potentials $U(r)$ (i.e. without a Coulomb tail). As shown in

[11, 12], the position of plateau cutoffs in ATI/ATD and HHG is essentially independent of the spatial symmetry of an initial bound state and the shape of $U(r)$. Thus in this study we use the most tractable model for $U(r)$, the zero-range potential supporting a single bound state of energy $E_0 = -\hbar^2\kappa^2(2m)^{-1}$. For LAES, the ZRP model represents a time-dependent extension of the scattering length approximation [13] for low-energy, s-wave electron scattering (the case for which rescattering effects are most important) from atoms that have negative ions with s-electron ground states.

We describe the laser field in the dipole approximation by the electric vector $\mathbf{F}(t)$:

$$\mathbf{F}(t) = F\,\mathrm{Re}\{\mathbf{e}\,\mathrm{e}^{-\mathrm{i}\omega t}\}, \qquad \mathbf{e} = (\hat{\varepsilon} + \mathrm{i}\eta[\hat{\mathbf{k}} \times \hat{\varepsilon}])/\sqrt{1+\eta^2}, \qquad -1 \leqslant \eta \leqslant +1,$$

where F, ω, and $\mathbf{e}$ are the amplitude, frequency, and complex polarization vector. (Thus with our definitions the laser intensity, $I = cF^2/(8\pi)$, is independent of the ellipticity η.) Unit vectors $\hat{\boldsymbol{\varepsilon}}$ and $\hat{\mathbf{k}}$ define respectively, the major semiaxis of the polarization ellipse and the direction of the laser beam. The ellipticity η is connected with the degrees of linear (ℓ) and circular (ξ) polarization as follows: $\ell = (1 - \eta^2)/(1 + \eta^2)$, $\xi = 2\eta/(1 + \eta^2)$. Since $|E_0|$ is the only free parameter of the problem in our approach, we use below scaled units in which the electron energies and $\hbar\omega$ are measured in units of $|E_0|$, momenta in units of $\hbar\kappa$ and field amplitudes in units of $F_0 = \sqrt{2m|E_0|^3}/(e\hbar)$.

The remarkable advantage of a ZRP model is that it allows one to represent the exact quasienergy solutions $\Phi(\mathbf{r}, t)$ of the time-dependent Schrödinger equation for both bound state and scattering problems (as well as the corresponding transition amplitudes) in terms of the free-electron (Volkov) Green function and a time-periodic function $f(t)$ that enters the boundary condition for $\Phi(\mathbf{r}, t)$ at the origin:

$$\lim_{r\to 0} \Phi(\mathbf{r}, t) = (r^{-1} - 1) f(t). \tag{1}$$

The functions $f(t)$ are different for quasistationary quasienergy states (QQESs) $\Phi_\epsilon(\mathbf{r}, t)$ with complex quasienergies, $\epsilon = \mathrm{Re}\,\epsilon - \mathrm{i}(\Gamma/2)$, and for scattering states $\Phi_{\mathbf{p}}(\mathbf{r}, t)$ with real quasienergies, $\epsilon = p^2 + u_p$, where $\mathbf{p}$ is the incoming electron momentum. We distinguish $f(t)$ for these two cases by $f_\epsilon(t)$ and $f_{\mathbf{p}}(t)$, respectively; they contain the complete information on the binding (for ATD and HHG) and scattering potential (for LAES) effects and play a key role in our analyses. The exact quantum results for the LAES and ATD amplitudes involve a sum of generalized Bessel functions multiplied by the Fourier-coefficients of $f(t)$ [3, 10]. For our purposes, it is convenient to represent these amplitudes in an equivalent form in terms of the following Fourier integral:

$$\mathcal{A}_n = \frac{1}{T}\int_0^T c^*_{\mathbf{p}_n}(t)\, f(t)\, \mathrm{e}^{\mathrm{i}n\omega t}\,\mathrm{d}t, \tag{2}$$

where $c_{\mathbf{p}_n}(t)$ is the periodic (in time) part of the Volkov wavefunction at the origin,

$$c_{\mathbf{p}_n}(t) = \exp\left[-\mathrm{i}\int^t (\mathbf{p}_n + \mathbf{A}(t'))^2\,\mathrm{d}t' + \mathrm{i}\left(p_n^2 + u_p\right)t\right],$$

and where $\mathbf{A}(t) = \dot{\mathbf{F}}(t)/\omega^2$, $u_p = F^2/(2\omega^2)$ and $\mathbf{p}_n$ is a final (detached or scattered) electron momentum. As shown by an accurate quantum analysis of our exactly solvable 3D-model, plateau features in strong field phenomena originate from those occurring in the spectra of the Fourier-coefficients of $f(t)$, or, equivalently, of the Fourier-harmonics of $\Phi(\mathbf{r}, t)$ near the origin (cf (1)). Thus, below we shall analyse the plateau features for the function $f_\epsilon(t)$ first, before considering the elliptical polarization cutoff laws for HHG and ATI processes.

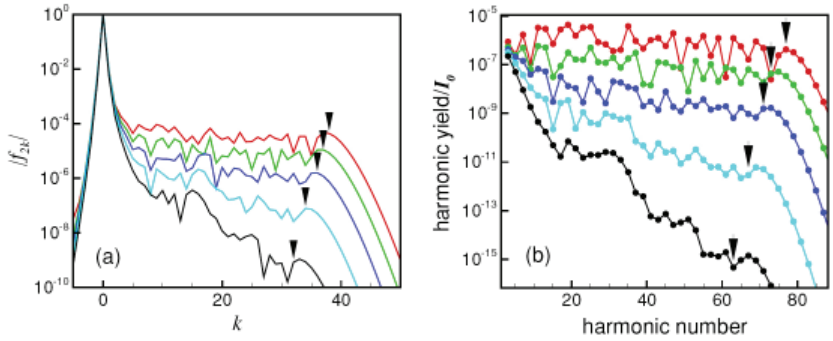

Figure 1. (a) Plateaux in the spectrum of the Fourier-coefficients f_{2k} for $F = 0.3$, $\omega = 0.128$, and five different values of ℓ (from top to bottom): 1.0, 0.923, 0.835, 0.724, 0.6. Arrows show the cutoffs given by equation (12). (b) Harmonic yield as a function of the harmonic number for the same values of F, ω, and ℓ as in panel (a). Arrows show the cutoffs given by equation (13). $I_0 = (2|E_0|^3e^2)/(3\hbar^2c^3)$.

(i) *Plateau features in the spectrum of the Fourier-coefficients of* $f_\epsilon(t)$. For bound state problems such as ATD or HHG, the complex quasienergy ϵ and the Fourier-coefficients f_{2k} of the QQES wavefunction $\Phi_\epsilon(\mathbf{r}, t)$ at the origin,

$$f_\epsilon(t) = \sum_k f_{2k} \exp(-2ik\omega t), \tag{3}$$

satisfy a homogeneous system of linear equations [14]:

$$\zeta_k(\epsilon) f_{2k} = \sum_{k' \neq k} M_{kk'}(\epsilon) f_{2k'}, \qquad \zeta_k(\epsilon) = \sqrt{u_p - \epsilon - 2k\omega} - 1 - M_{kk}(\epsilon). \tag{4}$$

The matrix elements $M_{kk'}(\epsilon)$ involve an integral containing Bessel functions $J_p(x)$:

$$\begin{aligned} M_{kk'}(\epsilon) &= \mathrm{i}^{k-k'} \sqrt{\frac{\omega}{4\pi \mathrm{i}}} \int_0^\infty \frac{\mathrm{d}\tau}{\tau^{3/2}} \mathrm{e}^{\mathrm{i}[k+k'+(\epsilon-u_p)/\omega]\tau} [\mathrm{e}^{\mathrm{i}\lambda(\tau)} J_{k-k'}(\ell z(\tau)) - \delta_{k,k'}], \\ z(\tau) &= \frac{u_p}{\omega}\left(\sin\tau - \frac{4\sin^2(\tau/2)}{\tau}\right), \qquad \lambda(\tau) = \frac{4u_p}{\omega}\frac{\sin^2(\tau/2)}{\tau}. \end{aligned} \tag{5}$$

The algorithms for direct numerical solution of the system (4) are discussed in [10]. In figure 1(a) we present the typical plateau-like behaviour (for positive k) of the coefficients f_{2k} for different values of ℓ (note that $f_{2k} \sim \ell^{2|k|}$ at $\ell \to 0$ (or $\xi \to \pm 1$)).

To estimate the cutoff in the spectrum of f_{2k} analytically, we use the 'rescattering approximation' [10] for f_{2k} (i.e. the first iteration of system (4) assuming

$$f_{2k}^{(1)} = \frac{M_{k0}(\epsilon = -1)}{\zeta_k(\epsilon = -1)}. \tag{6}$$

The approximation (6) is very accurate for an intense low-frequency field $\mathbf{F}(t)$ [10]. Since the parameter ζ_k depends smoothly on k, the k-dependence of the coefficients f_{2k} is dominated by that of the matrix elements $M_{k0}(\epsilon = -1)$. To estimate these matrix elements, we note first that the argument $z(\tau)$ of the Bessel function in (5) has maxima and minima at $\tau = \tau_n$, $n = 1, 2, \ldots$, where τ_n are roots of the equation [4]:

$$(2/\tau_n)\sin(\tau_n/2) - \cos(\tau_n/2) = \pm\sin(\tau_n/2). \tag{7}$$

The upper bound of $|z(\tau)|$ is given by its value for the lowest τ_n (i.e. $\tau_1 = 4.086$):

$$z_1 \equiv z(\tau_1) = -2(u_p/\omega)\sin^2(\tau_1/2) = -1.5866(u_p/\omega), \qquad \ddot{z}(\tau_1) = -(u_p/\omega)\sin\tau_1. \tag{8}$$

For our purposes, it is necessary to estimate the matrix element M_{k0} for large k: $k > \ell|z_1|$ (where $\ell|z_1| \gg 1$ for small ω and $\ell u_p \gg \omega$). For these parameter values, the Bessel function in (5) may be replaced by its Debye asymptotic limit [15]:

$$J_k(|x|) \approx \frac{e^{|x|\sqrt{\chi^2-1}}\left(\chi - \sqrt{\chi^2-1}\right)^k}{\sqrt{2\pi|x|}(\chi^2-1)^{1/4}}, \qquad \chi = \frac{k}{|x|}. \tag{9}$$

Since $|J_k(\ell z(\tau))|$ has a global maximum at $\tau = \tau_1$, the dominant contribution of $J_k(\ell z(\tau))$ to the integral in (5) comes from the small interval of τ centred at $\tau = \tau_1$. Substituting in (9) $x \to \ell z(\tau)$ and expanding $z(\tau)$ up to second-order terms near the point $\tau = \tau_1$, we obtain the following approximation for the Bessel function in (5):

$$J_k(\ell z(\tau)) \approx J_k(\ell z_1)\exp(-\beta(\tau - \tau_1)^2), \tag{10}$$

where $\beta = |\ddot{z}(\tau_1)|(2|z_1|)^{-1}\sqrt{k^2 - \ell^2 z_1^2} \approx k|\ddot{z}(\tau_1)|(2|z_1|)^{-1}$. Using (10) to evaluate the integral in (5) for $k' = 0$, the resulting approximate value for $|M_{k0}|$ is

$$|M_{k0}(\epsilon = -1)| \approx \sqrt{\frac{\omega}{4\beta\tau_1^3}}|J_k(\ell z_1)|\, e^{-\frac{\alpha^2}{4\beta}}, \tag{11}$$

where $\alpha = k - |z_1| - \omega^{-1}$. The approximation represented by (11) and (6) provides numerical results for $|f_{2k}|$ that are in excellent agreement with those calculated using the exact equation (4) for k values around the cut-off and beyond the plateau region. An analytical estimate for k_c corresponding to the cut-off in the spectrum of $|f_{2k}|$ may be deduced by estimating the maximum of $|M_{k0}|$ in (11) as a function of k (cf [4]). The position of this maximum may be estimated as the average of k_b and k_e, $k_{\max} \equiv k_c = (k_b + k_e)/2$, where $k_b \approx \ell|z_1|$ corresponds to the maximum of the Bessel function in (11) and $k_e \approx |z_1| + \omega^{-1}$ corresponds to the maximum of the exponential in (11). Thus we obtain the following result for k_c:

$$k_c \approx \frac{1 + 1.5866(1+\ell)u_p}{2\omega}, \tag{12}$$

which agrees well with the exact numerical results for the cut-off positions in figure 1(a) for $\ell \geq 0.6$ (or, equivalently, for $|\eta| \leq 0.5$).

(ii) *HHG*. Proceeding to the analysis of plateau cut-offs in HHG spectra, we note the similarity of plateau structures for f_{2k} in figure 1(a) to those in figure 1(b) for the harmonic yield (calculated using the exact quantum results for the HHG amplitude in a ZRP model [16]). Moreover, each cut-off for a given ℓ in figure 1(b) (i.e. the energy, $E^{(h)}_{\max}$, that corresponds to a maximum of the harmonic yield in the region of the plateau cut-off) is reasonably described by the following formula (except for $\ell = 0.6$, in which case the high-energy plateau almost vanishes and the harmonic yield is nine orders less than for $\ell = 1$):

$$E^{(h)}_{\max} \approx 1 + 1.5866(1+\ell)u_p, \tag{13}$$

which is equivalent to (12). This coincidence is not surprising and has a simple physical interpretation owing to the fact that the coefficient f_{2k} determines the population of the $(2k)$th Fourier-harmonic of the QQES $\Phi_\epsilon(\mathbf{r}, t)$ at the origin (see (1)), i.e. it is proportional to the amplitude for the electron having the energy $E_{2k} = \mathrm{Re}\,\epsilon + 2k\omega \approx E_0 + 2k\omega$. According to (12), a strong laser field effectively populates only the Fourier-harmonics of $\Phi_\epsilon(\mathbf{r}, t)$ near the origin having k up to $k \approx k_c$, from which the electron can emit (spontaneous) harmonic photons having a maximum energy $E^{(h)}_{\max} = E_{2k_c} - E_0 \approx 1 + 1.5866(1+\ell)u_p$. Note, that the estimate (13) was already obtained earlier [4] based on a straightforward evaluation of an approximate expression for the HHG amplitude in the complex quasienergy approach for a ZRP model. (It is interesting that in [4] all coefficients f_{2k} were neglected except for $f_0 = 1$. However, the re-

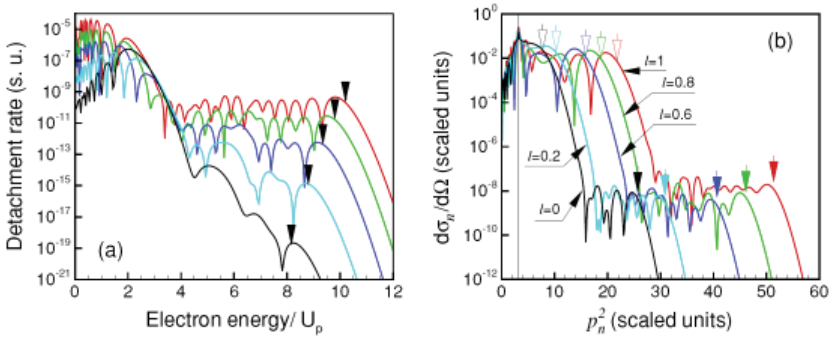

Figure 2. (a) ATD spectra of electrons ejected along the major polarization axis for the same laser parameters F, ω, and ℓ as in figure 1(a). Arrows indicate the cutoffs given by (15). (b) Energy distribution of scattered electrons (for forward scattering along the major axis of the polarization ellipse) for $F = 0.5$, $\omega = 0.155$, $E = 3.1775 = 20.5\omega = 0.61u_p$, and for different values of ℓ (indicated in figure). Hollow and filled vertical arrows show the *K*- and *R*-plateau cutoffs given respectively by (19) and (21), (22). The vertical line corresponds to the case of elastic scattering, $p^2{}_n = E$.

sulting HHG amplitude has a form similar to that of the matrix element $M_{k0}(\epsilon = -1)$, thus yielding the same cutoff as in (12).) The high accuracy of the estimate (13) for the case of linear polarization has been demonstrated in the experiment of [17]. We note that the estimate (12) has been obtained under the condition $\ell u_p \gg \omega$; thus the cut-off law (13) as well as that for ATD (see (15) below) cannot be employed for laser polarizations very close to circular (in which case $f_{2k} = f_0\delta_{k0}$ [14], HHG is impossible and plateau structures in ATI/ATD disappear).

(iii) *ATD*. Substituting the Fourier-expansion (3) into (2) (where $p_n = \sqrt{n\omega - 1 - u_p}$), the ATD amplitude $\mathcal{A}_n$ is expressed in terms of a coherent sum of contributions from separate coefficients f_{2k} multiplied by generalized Bessel functions [10]. Owing to the plateau-like behaviour of f_{2k}, in order to obtain an analytical estimate for the high-energy cutoff in the ATD spectrum we therefore assume that only the coefficient f_{2kc} gives the dominant contribution to the amplitude $\mathcal{A}_n$ in (2) for values of n near the cut-off of the high-energy plateau. (We have confirmed numerically that the addition of coefficients f_{2k} with $k < k_c$ does not change the estimates below.) Then, replacing the function $f\epsilon(t)$ by a single harmonic, $f_\epsilon(t) \sim \exp(-2ik_c\omega t)$, we handle the integral over t in (2) using the saddle point method, where the saddle points t_s are given by

$$(\mathbf{p}_n + \mathbf{A}(t_s))^2 = 1.5866(1 + \ell)u_p. \tag{14}$$

The maximum value of p_n corresponds to the minimum real value of t_s. For electron ejection along the major axis of the polarization ellipse, $p_{n,\max}$ is given by

$$\left(p_{n,\max} - \sqrt{\frac{1+\ell}{2}}\frac{F}{\omega}\right)^2 \approx 1.5866(1 + \ell)u_p \quad \text{or} \quad E_{n,\max} \approx 5.1(1 + \ell)u_p. \tag{15}$$

As shown in figure 2(a), the estimate (15) agrees reasonably well with the exact results for a ZRP model (calculated similarly to those in [18]; note that, e.g., for Kr ($|E_0| \approx 14.0$ eV) these results as well as those in figure 1 correspond to $\omega \approx 1.79$ eV and $I \approx 3.5 \times 10^{15}$ W cm^{-2}). The rapid decrease of the average plateau heights in figure 2(a) with decreasing ℓ originates from the similar decrease of f_{2k} in figure 1(a).

(iv) *LAES*. Similar to the QQES case, the exact scattering state $\Phi_{\mathbf{p}}(\mathbf{r}, t)$ of an electron with an initial momentum $\mathbf{p}$ in a ZRP model is essentially determined by its boundary condition (1)

at the origin [3] (with $f(t) \equiv f_{\mathbf{p}}(t)$). For our purposes, it is convenient to re-write the inhomogeneous system of linear equations for the Fourier-coefficients of $f_{\mathbf{p}}(t)$ (see [3]) in terms of an inhomogeneous integral equation:

$$(1 + \mathrm{i}p)\, f_{\mathbf{p}}(t) + c_{\mathbf{p}}(t) = -\frac{1}{\sqrt{4\pi\,\mathrm{i}}} \int_0^\infty \frac{\mathrm{d}\tau}{\tau^{3/2}}\, \mathrm{e}^{\mathrm{i}p^2\tau} (f_{\mathbf{p}}(t-\tau)\, \mathrm{e}^{\mathrm{i}u_p\tau + \mathrm{i}S(t,t-\tau)} - f_{\mathbf{p}}(t)), \tag{16}$$

where

$$S(t, t-\tau) = -\int_{t-\tau}^{t} \mathbf{A}(t')^2\, \mathrm{d}t' + \frac{1}{\tau}\left(\int_{t-\tau}^{t} \mathbf{A}(t')\, \mathrm{d}t'\right)^2.$$

Once $f_{\mathbf{p}}(t)$ is known, the exact amplitude $\mathcal{A}_n$ [3] for LAES with absorption ($n > 0$) or emission ($n < 0$) of $|n|$ photons may be recovered according to equation (2), in which the scattered electron momentum is $p_n = \sqrt{n\omega + p^2}$.

Let us consider first the iterative solution for $f_{\mathbf{p}}(t)$, neglecting the rhs of (16):

$$f_{\mathbf{p}}(t) \approx f_{\mathbf{p}}^{(0)}(t) = -\frac{c_{\mathbf{p}}(t)}{1 + \mathrm{i}p}. \tag{17}$$

As shown in [3], this result is equivalent to the Kroll-Watson (low-frequency) approximation [19] and describes the low-energy part (the 'K-plateau') of the electron spectrum. Using (17), the integral over t in the amplitude (2) may be estimated by the saddle point method, where the saddle points, $t = t_i (i = 1, 2, \ldots)$, are given by

$$(\mathbf{p} + \mathbf{A}(t_i))^2 = (\mathbf{p}_n + \mathbf{A}(t_i))^2. \tag{18}$$

Analysis shows that the amplitude (2) oscillates as a function of n for real values of t_i and has an exponential smallness for complex t_i. Thus the position of the K-plateau cutoff corresponds to the minimum value of p_n at which the roots t_i of equation (18) acquire an imaginary part. The extent of the K-plateau reaches a maximum when the vectors $\mathbf{p}$ and $\mathbf{p}_n$ are collinear with the major axis of the polarization ellipse:

$$p_{n,\max} = 2\sqrt{(1+\ell)u_p} \mp p, \qquad p_n > p, \tag{19}$$

where the signs $\mp$ correspond to parallel/antiparallel directions of $\mathbf{p}$ and $\mathbf{p}_n$. Thus, for the case of backscattering, the low-energy K-plateau exists for any p, while for forward scattering it exists only for incoming electron energies $E = p^2$ less than $(1 + \ell)u_p$ and its maximum extent, $E_{n,\max} = 4(1 + \ell)u_p$, is reached at $E \to 0$. (The analysis of the K-plateau cutoff for the case of nonzero scattering angle θ between $\mathbf{p}_n$ and $\mathbf{p}$ in the plane of the polarization ellipse has been presented in [7].)

The analysis of the high-energy part of the electron spectrum requires a more exact account of the scattering potential corresponding to the next iteration of (16), $f_{\mathbf{p}}(t) \approx f^{(0)}{}_{\mathbf{p}}(t) + f^{(1)}{}_{\mathbf{p}}(t)$, in which (17) is substituted on the rhs of (16) to obtain

$$\begin{aligned} f_{\mathbf{p}}^{(1)}(t) &= \frac{1}{(1+\mathrm{i}p)^2\sqrt{4\pi\,\mathrm{i}}} \int_0^\infty \frac{\mathrm{d}\tau}{\tau^{3/2}} (\mathrm{e}^{\mathrm{i}[\varphi(t,\tau) + (E+u_p)t]} - c_{\mathbf{p}}(t)\, \mathrm{e}^{\mathrm{i}E\tau}), \\ \varphi(t,\tau) &= S(t, t-\tau) - \int^{t-\tau} (\mathbf{p} + \mathbf{A}(t'))^2\, \mathrm{d}t'. \end{aligned} \tag{20}$$

For low frequencies, the integrals over τ in (20) as well as over t in (2) may be evaluated using the saddle point method. The saddle points in the plane of τ, $\tau_s = \tau_s(t) (s = 1, 2, \ldots)$, are given by equation

$$(\mathbf{p} + \mathbf{A}(t - \tau_s))^2 = (\mathbf{k}(t, \tau_s) + \mathbf{A}(t - \tau_s))^2, \qquad \mathbf{k}(t, \tau_s) = -\frac{1}{\tau_s} \int_{t-\tau_s}^{t} \mathbf{A}(t')\, \mathrm{d}t', \tag{21}$$

while those in the t-plane, $t = t_f (f = 1, 2, ...)$, are given by (see [7] for details)

$$(\mathbf{k}(t_f, \tau_s(t_f)) + \mathbf{A}(t_f))^2 = (\mathbf{p}_n + \mathbf{A}(t_f))^2. \tag{22}$$

As for the case of the K-plateau, the rescattering (R) plateau corresponds to the values of $\mathbf{p}_n$ for which there exist real solutions of equations (21) and (22), i.e. the cutoff of the R-plateau is given by the minimum value of p_n at which the roots t_f and τ_s become complex. For the cases of $\ell = 1$ and $\ell = 0$, equations (21) and (22) reduce to a single equation involving only the roots τ_s, so that the cutoff value of p_n may be obtained by maximizing $p_n(p, \theta, \tau_s)$ over the set of τ_s (for given p, θ and laser parameters). For forward scattering ($\theta = 0$) either along the laser polarization (for $\ell = 1$) or in the polarization plane (for $\ell = 0$), the cutoff value of p_n is given by [3, 7]

$$p_{n,\max} = \begin{cases} \sqrt{u_p}\max\left(\dfrac{a(\zeta^2 - \upsilon^2) - 2\zeta\upsilon\sqrt{8(\zeta^2 + \upsilon^2) - a^2}}{\zeta^2 + \upsilon^2}\right), & \ell = 1 \\ \sqrt{u_p}\,\max(\sqrt{c(\phi) + \sin^2\psi(\phi)} - \sin\psi(\phi)), & \ell = 0, \end{cases} \tag{23}$$

where $a = p/\sqrt{u_p}$, $\phi = \omega\tau_s$,

$$\zeta = \tfrac{1}{\phi}\sin\tfrac{\phi}{2} - \cos\tfrac{\phi}{2}, \qquad \upsilon = \sin\tfrac{\phi}{2},$$
$$c(\phi) = \tfrac{4\zeta\upsilon}{\phi}, \qquad \psi(\phi) = \phi - \arcsin\tfrac{a^2 - c(\phi)}{2a}.$$

The energy spans of the K and R-plateaux depend significantly on the energy $E = p^2$ and the laser polarization. For linear polarization and forward scattering, the extent of each plateau is maximal at $p \to 0$, with the maximum extent of the R-plateau being $E_{n,\max} \approx 10.2u_p$ (as in equation (15) for ATD). $E_{n,\max}$ decreases with increasing E and the R-plateau disappears at $E \approx 10.2u_p$ [3]. Our numerical analysis for circular polarization and forward scattering shows that the R-plateau is masked at low energies by the more intense K-plateau, becoming visible only for energies $E \geq 0.03u_p$. With increasing E, its extent becomes maximal ($E_{n,\max} \approx 5.1u_p$) for $E \approx 0.2u_p$ and thereupon decreases smoothly to $\approx 4.1u_p$ for $E \approx 4.1u_p$. For $E \geq 4.1u_p$, the R-plateau for circular polarization vanishes. (For nonzero scattering angles θ, the extent of the R-plateau depends upon the sign of ξ (a circular dichroism effect) [7].)

In figure 2(b) we present the energy distribution of electrons for forward scattering along the major polarization axis (calculated using the exact results [3] for the scattering amplitude $\mathcal{A}_n$), where the vertical arrows indicate the cutoff positions given by equations (19), (21) and (22). (For e^- H scattering, these results correspond to an incoming electron energy of 2.4 eV and a CO_2 laser field ($\lambda = 10.6$ μm) of intensity 3.7×10^{11} W cm^{-2}.) Although the exact dependence (according to (21), (22)) of the R-plateau cutoff position on ℓ is nonlinear, our numerical analysis shows that it is fairly well approximated by the following interpolation formula:

$$E_{n,\max}(\ell) = \ell E_{n,\max}^{(\ell=1)} + (1 - \ell)E_{n,\max}^{(\ell=0)}, \tag{24}$$

where $E^{(\ell)}_{n,\max} = [p^{(\ell)}_{n,\max}]^2$ and $p^{(\ell=1)}_{n,\max}$ and $p^{(\ell=0)}_{n,\max}$ are given by (23). In particular, for $\ell = 0.8$, 0.6 and 0.2 in figure 2(b), the exact cutoffs ($p^2_n = 46.11$, 41.01, and 30.84) are almost indistinguishable from those given by (24) ($p^2_n = 46.14$, 41.06, and 30.89). The most spectacular feature of the high-energy plateau for LAES compared to those for HHG and ATD in figures 1(b) and 2(a) is that its height (but not its length!) is almost independent of the ellipticity, including for the case of pure circular polarization.

In conclusion, we have obtained analytical estimates for the ellipticity dependence of high-energy plateau cutoffs for the most fundamental intense laser-atom processes based on rigorous quantum results for transition amplitudes within the quasienergy approach (and their

low-frequency analysis). For the case of linear polarization, the cutoff positions coincide with predictions of classical and semiclassical simulations based on the widely known rescattering scenario [20–22]. Thus our results provide a quantum justification of the rescattering picture as well as its extension to the case of an arbitrary laser polarization including (for LAES) the intriguing case of circular polarization. Indeed, equations (21), (22) have a transparent classical interpretation in terms of rescattering. First, the relation (18) describes LAES as a single collisional event at the origin, in which an incoming electron instantly changes its momentum from $\mathbf{p}$ to $\mathbf{p}_n$ at a certain moment, $t = t_i$, governed by the conservation of energy for the incoming and scattered electrons (i.e. equality of the lhs and rhs of (18), respectively). In contrast, equations (21) and (22) correspond to the two-step (rescattering) scenario of LAES, which involves an intermediate state with electron momentum $\mathbf{k}$. Namely, at the time $t_i = t_f - \tau_s$ the incoming electron changes its momentum from $\mathbf{p}$ to $\mathbf{k}$ (see (21)), so that after time τ_s the electron can be returned by the elliptically polarized laser field to the origin, where at the time $t_f = t_i + \tau_s$ it acquires the final momentum $\mathbf{p}_n$ at the second collisional event (see (22)).

Acknowledgments

This work was supported in part by NSF Grant PHY-0300555, by RFBR Grant 04-02-16350 and by the joint Grant VZ-010-0 of the CRDF and the RF Ministry of Education. AVF acknowledges support of the "Dynasty" Foundation.

References

[1] Protopapas M, Keitel C H and Knight P L 1997 *Rep. Prog. Phys.* **60** 389
[2] Becker W, Grasbon F, Kopold R, Milosevic D B, Paulus G G and Walther H 2002 *Adv. At. Mol. Opt. Phys.* **48** 35
[3] Manakov N L, Starace A F, Flegel A V and Frolov M V 2002 *Piz. Zh. Eksp. Teor. Fiz.* **76** 316; Manakov N L, Starace A F, Flegel A V and Frolov M V 2002 *JETP Lett.* **76** 256 (Engl. Transl.)
[4] Becker W, Long S and McIver J K 1994 *Phys. Rev.* A **50** 1540
[5] Milosevic D B 2000 *J. Phys. B: At. Mol. Opt. Phys.* **33** 2479
[6] Kopold R, Milosevic D B and Becker W 2000 *Phys. Rev. Lett.* **84** 3831
[7] Flegel A V, Frolov M V, Manakov N L and Starace A F 2004 *Phys. Lett.* A at press
[8] Manakov N L, Ovsiannikov V D and Rapoport L P 1986 *Phys. Rep.* **141** 319
[9] Manakov N L, Frolov M V, Starace A F and Fabrikant I I 2000 *J. Phys. B: At. Mol. Opt. Phys.* **33** R141
[10] Manakov N L, Frolov M V, Borca B and Starace A F 2003 *J. Phys. B: At. Mol. Opt. Phys.* **36** R49
[11] Frolov M V, Manakov N L, Pronin E A and Starace A F 2003 *Phys. Rev. Lett.* **91** 053003
[12] Milosevic D B, Gazibegovic-Busuladzic A and Becker W 2003 *Phys. Rev.* A **68** 050702(R)
[13] Landau L L and Lifshitz E M 1992 *Quantum Mechanics* 4th edn (Oxford: Pergamon) section 133
[14] Manakov N L and Fainshtein A G 1980 *Zh. Eksp. Teor. Fiz.* **79** 751; Manakov N L and Fainshtein A G 1980 *Sov. Phys. - JETP* **52** 382 (Engl. Transl.)
[15] 1965 *Handbook of Mathematical Functions* ed Abramowitz M Stegun I A (New York: Dover) equation (9.3.7)
[16] Borca B, Flegel A V, Frolov M V, Manakov N L and Starace A F 2002 *Phys. Rev.* A **65** 051402(R)
[17] Papadogiannis N A, Kalpouzos C, Witzel B, Fotakis C and Charalambidis D 2000 *J. Phys. B: At. Mol. Opt. Phys.* **33** L79
[18] Borca B, Frolov M V, Manakov N L and Starace A F 2002 *Phys. Rev. Lett.* **88** 193001
[19] Kroll N M and Watson K M 1973 *Phys. Rev.* A **8** 804
[20] Kuchiev M Yu 1987 *Piz. Zh. Eksp. Teor. Fiz.* **45** 319; Kuchiev M Yu 1987 *JETP Lett.* **45** 404 (Engl. Transl.)
[21] Kulander K C, Schafer K J and Krause J L 1993 *Super-Intense Laser-Atom Physics (NATO ASI Series B: Physics vol 316)* ed B Piraux *et al* (New York: Plenum) p 95
[22] Corkum P B 1993 *Phys. Rev. Lett.* **71** 1994